

BIS Brazilian Dental Science

25th Jubilee



Source: macrovector/Freepik



Magnetic resonance imaging texture analysis of the temporomandibular joint for changes in the articular disc in individuals with migraine headache

Análise de textura por ressonância magnética da articulação temporomandibular com alterações no disco articular em indivíduos com cefaleia migrânea

Karolina Aparecida Castilho FARDIM¹ , Thais Mara Aparecida Monfredini RIBEIRO¹ , Elaine Cristina de Carvalho Beda Correa de ARAÚJO¹ , Celso Massahiro OGAWA² , Andre Luiz Ferreira COSTA² , Sérgio Lucio Pereira de Castro LOPES¹

1 - Departamento de Diagnóstico e Cirurgia, Faculdade de Odontologia de São José dos Campos, Universidade Estadual Paulista (UNESP), São José dos Campos, SP, Brazil.

2 - Programa de Pós-Graduação em Odontologia, Universidade Cruzeiro do Sul (UNICSUL), São Paulo, Brazil.

How to cite: Fardim KAC, Ribeiro TMAM, Araújo ECCBC, Ogawa CM, Costa ALF, Lopes SLPC. Magnetic resonance imaging texture analysis of the temporomandibular joint for changes in the articular disc in individuals with migraine headache. *Braz Dent Sci*. 2023;26(1):e3649. <https://doi.org/10.4322/bds.2023.e3649>

ABSTRACT

Objective: the aim of this study was to analyse the performance of the technique of texture analysis (TA) with magnetic resonance imaging (MRI) scans of temporomandibular joints (TMJs) as a tool for identification of possible changes in individuals with migraine headache (MH) by relating the findings to the presence of internal derangements. **Material and Methods:** thirty MRI scans of the TMJ were selected for study, of which 15 were from individuals without MH or any other type of headache (control group) and 15 from those diagnosed with migraine. T2-weighted MRI scans of the articular joints taken in closed-mouth position were used for TA. The co-occurrence matrix was used to calculate the texture parameters. Fisher's exact test was used to compare the groups for gender, disc function and disc position, whereas Mann-Whitney's test was used for other parameters. The relationship of TA with disc position and function was assessed by using logistic regression adjusted for side and group. **Results:** the results indicated that the MRI texture analysis of articular discs in individuals with migraine headache has the potential to determine the behaviour of disc derangements, in which high values of contrast, low values of entropy and their correlation can correspond to displacements and tendency for non-reduction of the disc in these individuals. **Conclusion:** the TA of articular discs in individuals with MH has the potential to determine the behaviour of disc derangements based on high values of contrast and low values of entropy

KEYWORDS

Texture Analysis; Migraine disorders; Temporomandibular disorders; Radiomics; Temporomandibular Joint Disc.

RESUMO

Objetivo: o objetivo deste estudo foi analisar o desempenho da técnica de análise de textura (AT) em exames de ressonância magnética (RM) das articulações temporomandibulares (ATM) como ferramenta para identificação de possíveis alterações em indivíduos com cefaléia migrânea (CM) relacionando os achados com a presença de desarranjos internos. **Material e Métodos:** trinta exames de RM das ATM foram selecionados para estudo, sendo 15 de indivíduos sem cefaleia migrânea ou qualquer outro tipo de cefaléia (grupo controle) e 15 diagnosticados com CM. As imagens de RM ponderadas em T2 das articulações realizadas na posição de boca fechada foram usadas para AT. A matriz de co-ocorrência foi usada para calcular os parâmetros de textura. O teste exato de Fisher foi usado para comparar os grupos quanto ao sexo, função do disco e posição do disco, enquanto o teste de Mann-Whitney foi usado para os demais parâmetros. A relação da AT com a posição e função do disco foi avaliada por meio de regressão logística ajustada para lado e grupo. **Resultados:** a AT por RM dos discos articulares em

indivíduos com cefaleia migrânea tem o potencial de determinar o comportamento dos desarranjos discais, em que altos valores de contraste, baixos valores de entropia e sua correlação podem corresponder a deslocamentos e tendência a não redução do disco nesses indivíduos. **Conclusão:** a análise de textura dos discos articulares em indivíduos com CM tem potencial para determinar o comportamento dos desarranjos do disco com base em altos valores de contraste e baixos valores de entropia.

PALAVRAS-CHAVE

Transtornos da Cefaleia; Análise de Textura; Transtornos da Articulação Temporomandibular; Radiômica; Disco da Articulação Temporomandibular.

INTRODUCTION

The temporomandibular joint (TMJ) is a synovial articulation consisting of the condyle (mandibular head), tubercle (articular eminence) and mandibular fossa. These anatomical structures make the interaction between temporal bone at the skull base and the mandible, thus justifying why TMJ is also called craniomandibular joint [1].

Temporomandibular dysfunctions (TMDs) are considered changes in the masticatory muscles and TMJ, or both [2]. There is a significantly relevant number of patients with TMD-related disorders affecting directly their quality of life [3,4]. Moreover, these disorders are considered one of the most common chronic conditions of non-dental orofacial pain seen by dental surgeons and other healthcare professionals [5]. Patients with TMD can present several signs and symptoms, among them the most frequent are the following: pain in the TMJ region, headache, pain in the masticatory muscles, ear pain, facial pain, functional limitation, cervical pain, difficult mouth opening, pain during mastication, ear buzzing, mandibular pain, among others [6,7].

Headaches are very common chronic manifestations in our society as they can incapacitate the affected individuals by not allowing them to perform their daily activities, thus being considered a public health problem. They are classified into primary and secondary types, in which the former has an idiopathic origin as clinical and laboratory examinations cannot explain its aetiology. The so-called migraine headache (MH), popularly known as migraine, is an example of primary headache. As for the secondary headache, pain occurs in response to an injury, such as the tension headaches [8].

The tendency of an individual to have MH is associated with genetic bases. In this sense, a retrospective study [9] showed that MH is the most common disease related to TMD. There already exist studies correlating the presence of

internal derangement to MH, but none of them analysed objectively the structures of the TMJ components, such as the articular disc [10-12].

The imaging study of TMJ soft tissues, as is the case of the articular disc, can be performed with the gold-standard method, which consists of using magnetic resonance imaging (MRI) scans. MRI can determine the precise localisation of the articular joint [13], thus allowing the study of its position and shape so that possible changes can be identified, such as presence of disc displacement and internal derangements, which are defined as changes in the normal relationship between disc and bone components of the TMJ [14]. Additionally, MRI is a non-invasive technique as it is based on image acquisition by means of radiofrequency waves rather than of ionising radiation, thus having no deleterious effect on living organisms.

With the advance in the computing techniques, a method to quantify efficiently complex structures in images on a non-invasive basis has been developed by measuring the distribution of grey levels in the region of interest (ROI) delimited in the image. This technique is called texture analysis (TA). Prior studies used TA to characterise lesions in the several regions of the body and distinguish them from normal tissues, since pathological tissues present a greater heterogeneity in the parameters of texture [15-17].

The objective of this study was to use the TA in MRI scans as a tool to identify possible changes in the articular disc of the TMJ in individuals with MH due to internal derangements by comparing the values obtained to those in the control group of individuals without MH.

MATERIAL AND METHODS

All the steps of the study were carried out in the Radiology Clinics of the Department of Diagnosis and Surgery of the Paulista State University Dental School (UNESP) in São José dos

Campos, SP, Brazil. The study was approved by the local research ethics committee according to protocol number CAAE 32339720.8.0000.0077.

Fifteen MRI scans from individuals without MH or any other headache (Control Group) and 15 from individuals diagnosed with MH (Migraine Group) were selected for study. All the MRI scans are from the personal archive of the main researcher, which had been used in a previous study on MRI for analysis of MH [10]. The diagnosis of MH was made at the time of image acquisition by a neurologist, who followed the criteria of the International Classification of Headache Disorders criteria [18].

All the scans were acquired by using a MRI scanner 1.5 T (Sigma, General Electric, Milwaukee, WI, USA) with an 8-channel bilateral surface coils, in which parasagittal and lateral-medial images were obtained perpendicularly to the long axis of the mandibular head with mouth closed and maximum mouth opening. The same protocol was used for all image acquisitions as follows:

- T1: repetition time of 850 ms, echo time of 8.5 ms, section thickness of 3.0 mm, FOV of 150 x 150 mm and matrix of 512 x 512 pixels;
- T2: fat saturation: repetition time of 1500 ms, echo time of 100.2 ms, section thickness of 3.0 mm, FOV of 150 x 150 mm and matrix of 512 x 512 pixels;

Evaluation of the MRI scans was performed in two steps, in which presence of internal derangements (i.e. disc displacement and changes in the disc function) was determined first and then the TA of the discs was calculated.

The MRI scans were evaluated on a 19-inch monitor under reduced illumination by a previously trained examiner using the Merge eFilm Workstation software, version 1.5 (Merge Healthcare, Chicago, IL, USA).

The disc position was evaluated on images acquired with mouth closed and the disc function on images acquired with maximum mouth opening, according to the principles set by Tasaki et al. [19].

MRI TEXTURE ANALYSIS OF THE ARTICULAR DISCS

MRI texture analysis was performed by using MaZda software version 3.20 (Institute of

Electronics, Technical University of Lodz, Poland), which consists of a specific package for this purpose. The texture of articular discs was determined by using parasagittal sections of the T2-weighted images. Three consecutive sections corresponding to lateral, central and medial views were chosen. The reason for performing TA of T2-weighted images is that the normal articular disc presents hyposignal, whereas those with hypersignal indicate presence of liquid. In this way, a change in the articular disc generating a hypersignal in T2-weighted images reflects a region or tissue containing liquid, such as oedema and hydropic degeneration, which would involve intracellular accumulation of water (cell hyper-hydration) resulting from an imbalance in the osmotic gradient control in the cytoplasmic membrane and mechanisms of absorption and elimination of water and intracellular electrolytes [20].

In both experimental and control groups, each parasagittal section of the T2-weighted image acquired with closed mouth was exported in bitmap format (.bmp) before using the tool “draw polygon” of the MaZda software version 3.20 to delimitate the entire articular disc in order to determine the region of interest (ROI) for TA (Figure 1).

TA is based on the so-called co-occurrence matrix (COM) [21], which provides information on the spatial relationship between the pixels of the image within the ROI as determined by the operator. The MaZda software can make variations in the coordinates of the spatial relationship among elements of this matrix in order to determine the frequency of different information on the pixel values analysed. Therefore, this software allows selecting specific parameters whose meanings are used to interpret the behaviour of the tissue, thus providing values for TA.

Next, matrix parameters regarding the directions of the horizontal (horzl), vertical (vertl), 40-degrees (45 dgr) and 135-degrees (135 dgr) pixels were selected so that pixel values could be analysed in different spatial positions.

The values for each section were tabulated and a mean value of the three sections (i.e. lateral, central and medial) for each parameter was obtained by segmenting the disc before performing TA. This mean value corresponded to the value to be analysed so that values covering the whole extension of the disc could be obtained.

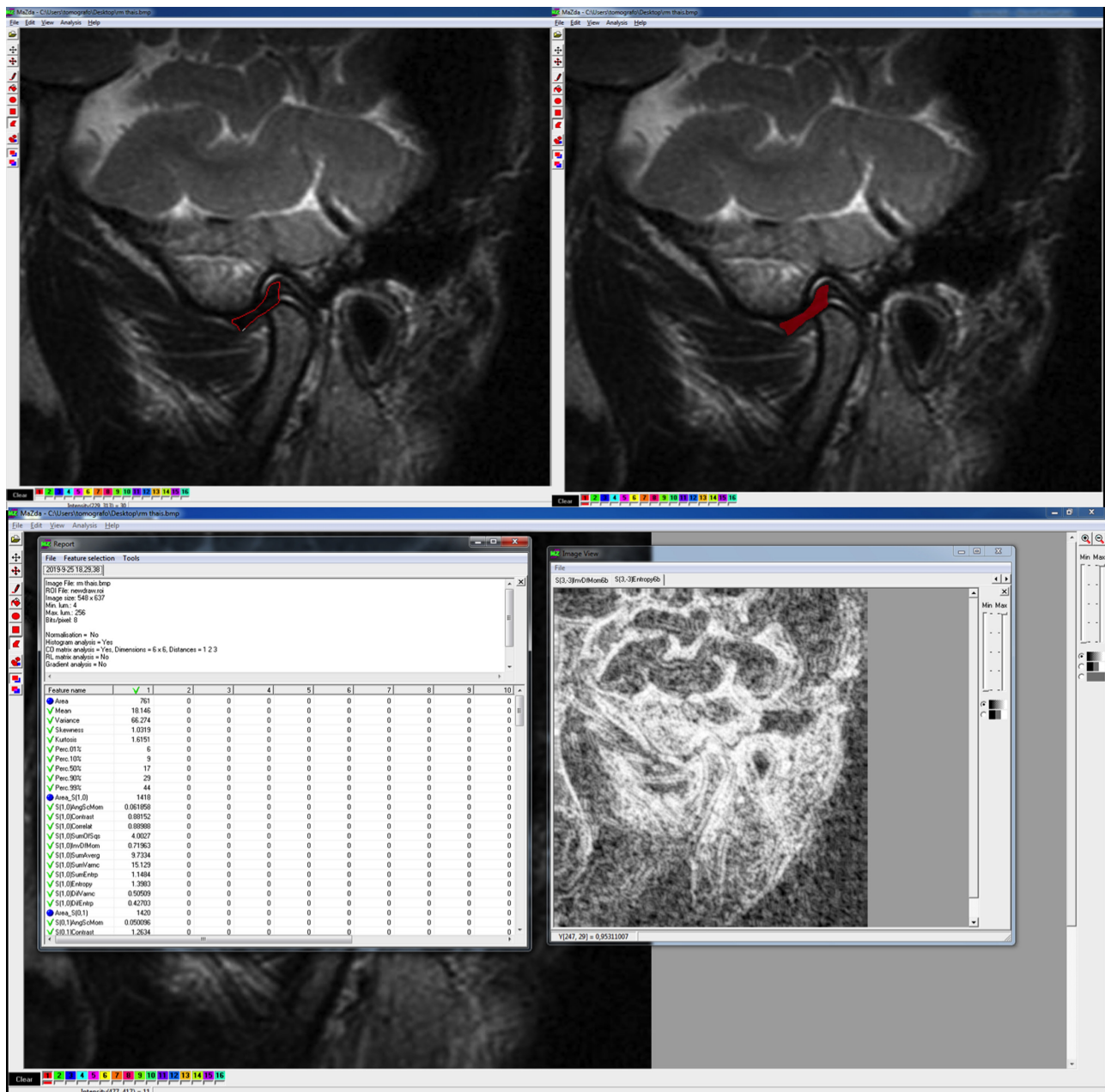


Figure 1 – Example of ROI delimitation of the articular disc in a T2-weighted image of the TMJ and calculation of texture parameters by using the MaZda software.

All the texture analyses were performed by a previously trained evaluator in the in the Radiology Clinics of the Department of Diagnosis and Surgery of the School of Dentistry of UNESP.

The examiner was calibrated as follows: the examiner performed the analyses of the position and function of the discs by using 20 MRI scans at intervals of 7 days. The resulting data were submitted to Kappa test and a concordance coefficient above 90% confirmed the examiner's calibration. The same procedure was performed for TA, with the resulting data being submitted to ICC test to be considered calibrated (90%).

Statistical analyses

Fisher's exact test was used to compare the groups regarding gender and disc's function and position, whereas Mann-Whitney test was used to compare the other parameters. The comparison between the groups was performed by side. The relationship of TA with disc's position and function was assessed by using logistic regression analysis adjusted for side and group. All statistical analyses were performed by using the software R, version 3.6.0 © (The R Foundation for Statistical Computing).

RESULTS

Thirty MRI scans of the TMJ were selected for study, of which 15 were from individuals without migraine (control group) and 15 from those diagnosed with migraine (migraine group). Control group had 11 (73.3%) females and the migraine group had 13 (86.7%) ones.

There was no difference between the groups regarding gender (P -value = 0.989; Fisher's exact test). There was also no significant difference between the groups regarding age (P -value = 0.651; Mann-Whitney test), with control and migraine groups having the same mean age of 42.7 years old.

Twelve different distances were evaluated by TA, with each distance having 11 parameters of texture, totalising 132 parameters. Considering the 30 MRI scans, there was a very great number of texture parameters being evaluated. Therefore, the following parameters were considered the most important: AngScMom (angular second moment), Contrast, Correlat (correlation), InvDfMom (inverse difference moment), SumOfSq (sum of squares), SumEntrp (sum of entropy) and Entropy. However, even if all directions were evaluated, there would be a very excessive number of variables given the

number of MRI scans in our sample. In this way, Spearman's correlation was calculated for all parameters and dimensions, in which parameters with correlation ≥ 0.75 or ≤ -0.75 in relation to other parameter were excluded, thus remaining 33 texture parameters in total.

Tables I-II present the descriptive measurements and the comparison between the groups on the right side. In Table I, one can observe the median, minimum and maximum values, including P -value in the comparison between the groups on the right side, whereas in Table II one can observe mean value and standard deviation of the texture parameters by group.

In Table I, one can observe that the migraine group presented more disc displacements (P -value = 0.009; Fisher's exact test) and more changes in disc function (non-reduced discs) (P -value = 0.007; Fisher's exact test). With regard to TA, the migraine group showed higher values for the parameters S10Contrast and S22Contrast as well as lower values for parameters S10Correlat and S11Correlat.

Figure 2 shows the texture parameters which presented statistically significant differences between control and migraine groups on the right side.

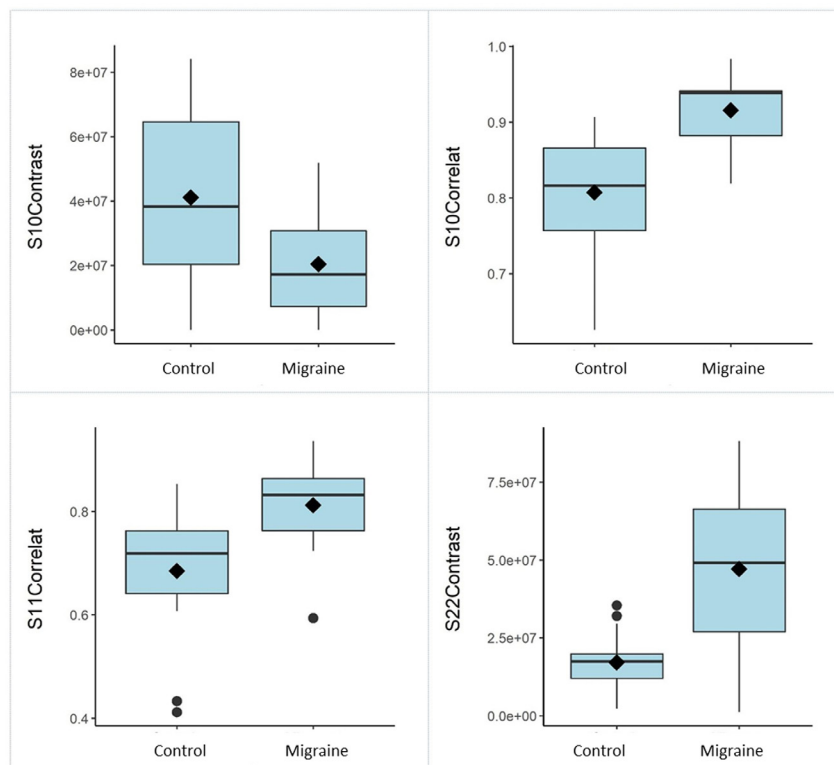


Figure 2 – Boxplots of the texture parameters which presented statistically significant difference between the groups on the right side.

Table I – Comparison between groups on the right side by using Fisher's exact test or Mann Whitney's test

Parameter	Right Side		P-value
	Control (N=15) Median [Min; Max]	Migraine (N=15) Median [Min; Max]	
Disc Position			0.009
Displaced	2 (13.3%)	10 (66.7%)	
Normal	13 (86.7%)	5 (33.3%)	
Disc Function			0.007
Non-reduced	1 (6.67%)	9 (60.0%)	
Reduced	14 (93.3%)	6 (40.0%)	
S10AngScMom	0.02 [0.01; 0.03]	0.03 [0.01; 0.10]	0.604
S10Contrast	38297872 [4.00; 84148936]	17234043 [0.53; 51808511]	0.019
S10Correlat	0.82 [0.63; 0.91]	0.94 [0.82; 0.98]	<0.001
S10SumOfSqs	20511883 [1889588; 88044364]	21913762 [1432874; 71523314]	0.820
S10SumEntrp	12912529 [1436964;14652918]	13511286 [0.99; 16572731]	0.330
S01Contrast	29791667 [15625; 72708333]	22395833 [0.94; 73854167]	0.171
S01Correlat	0.87 [0.72; 0.91]	0.81 [0.64; 0.93]	0.071
S01SumOfSqs	20970459 [208294; 88057454]	21399468 [151301;71484104]	0.820
S01SumEntrp	13104067 [1273463;14494688]	13139168 [0.98; 15742717]	0.494
S11Contrast	45666667 [4.00; 83444444]	18688889 [3.10; 90666667]	0.310
S11Correlat	0.72 [0.41; 0.85]	0.83 [0.59; 0.94]	0.002
S11SumOfSqs	23431451 [1782034; 90758025]	39192469 [1136284; 71902469]	0.917
S11Entropy	18378762 [1667239; 20110383]	17148857 [1592995; 21917217]	0.885
S1m1Contrast	30777778 [5.20; 96111111]	31688889 [0.83; 89777778]	0.852
S1m1Correlat	0.70 [0.31; 0.83]	0.72 [0.26; 0.82]	0.950
S1m1SumOfSqs	20729969 [2132034; 86888889]	22217284 [66275; 73521914]	0.694
S20Contrast	20037037 [1345679; 72222222]	18345679 [1437037; 63209877]	0.787
S20SumOfSqs	21879134 [1324036; 88148148]	22961439 [689148; 72130316]	0.633
S02Contrast	23505882 [4.60; 97176471]	41764706 [119; 92788235]	0.950
S02SumOfSqs	22071315 [1380955; 92804498]	19391349 [4776692; 72549827]	0.373
S22Contrast	17383562 [2209589; 35424658]	49109589 [1160274; 88219178]	0.001
S22SumOfSqs	22325389 [2064271; 95241603]	16858322 [2383374;72957262]	0.330
S2m2Contrast	16479452 [1490411; 62465753]	18219178 [22.0; 78835616]	0.663
S2m2SumOfSqs	19790814 [2032356; 68221055]	38733768 [11315538; 99713361]	0.093
S30Contrast	33264706 [10529412; 90441176]	32647059 [8.50; 85441176]	0.724
S30SumOfSqs	21988754 [12547362; 93122837]	35467939 [6642247; 98234753]	0.983
S03Contrast	17824324 [1177027; 78648649]	28783784 [10175676; 99351351]	0.101
S03SumEntrp	11126686 [136782; 14039459]	11764806 [0.82;14836123]	0.852
S33Contrast	23431034 [14017241; 53655172]	15931034 [4.50; 86948276]	0.229
S33SumOfSqs	20416394 [1602341; 69693074]	36524078 [4785003; 99912827]	0.237
S33SumEntrp	11951044 [0.82;13617913]	12976173 [0.78; 14739491]	0.110
S3m3Contrast	19482759 [26.0; 99137931]	24310345 [277; 95275862]	0.917
S3m3SumOfSqs	22726219 [1978478; 91964923]	25079518 [119919; 68456822]	0.663

Tables III-IV present the descriptive measurements and the comparison results regarding the left side. In Table III, one can observe the median, minimum and maximum values, including *P*-value in the comparison between the groups on the left side, whereas in Table IV one can observe the mean value and standard deviation of the texture parameters by group.

In Table III, one can observe that the migraine group presented more disc displacements (*P*-value = 0.002; Fisher's exact test) and more changes in

disc function (non-reduced discs) (*P*-value = 0.014; Fisher's exact test). With regard to TA, the migraine group showed higher values for the parameters S10Correlat, S10SumOfSqs, S01SumOfSqs, S11Correlat, S02SumOfSqs, S30SumOfSqs and S33Contrast as well as lower values for parameters S01Correlat and S1m1Correlat.

Figure 3 shows the texture parameters which presented statistically significant differences between control and migraine groups on the left side.

Table II – Mean and standard deviation of TA by group on the right side

Parameter	Right Side	
	Control (N=15) Mean (S.D.)	Migraine (N=15) Mean (S.D.)
S10AngScMom	0.02 (0.01)	0.03 (0.03)
S10Contrast	41104965 (26184884)	20439716 (17541999)
S10Correlat	0.81 (0.08)	0.92 (0.05)
S10SumOfSqs	33093818 (27563737)	32041355 (24999555)
S10SumEntrp	12462408 (3199419)	12401667 (5101838)
S01Contrast	29381514 (19830559)	22921703 (22523574)
S01Correlat	0.85 (0.06)	0.80 (0.08)
S01SumOfSqs	31391401 (27722097)	30805948 (25541016)
S01SumEntrp	10932826 (5026899)	11341142 (5607201)
S11Contrast	38031114 (31115973)	24497778 (21753120)
S11Correlat	0.68 (0.12)	0.81 (0.09)
S11SumOfSqs	35405483 (28279072)	35592885 (26475587)
S11Entropy	15343282 (7106420)	14870546 (7300256)
S1m1Contrast	38055557 (32444607)	36441482 (25002615)
S1m1Correlat	0.68 (0.12)	0.66 (0.16)
S1m1SumOfSqs	35598426 (26650193)	32915157 (23534763)
S20Contrast	24668066 (22584783)	22653416 (19304385)
S20SumOfSqs	35624008 (25997660)	32428396 (22565161)
S02Contrast	45674510 (36826003)	44759302 (30046573)
S02SumOfSqs	36406723 (27091603)	30146047 (23401706)
S22Contrast	17124475 (9586326)	47125571 (26058604)
S22SumOfSqs	35999944 (27651068)	29317819 (25151435)
S2m2Contrast	24704110 (17803459)	29171965 (24763984)
S2m2SumOfSqs	26364179 (21962415)	43401414 (27077348)
S30Contrast	37634314 (24973893)	36562748 (28643558)
S30SumOfSqs	35774917 (25005521)	38199236 (26858117)
S03Contrast	24928739 (21587368)	40134865 (30893439)
S03SumEntrp	9276817 (5316520)	9014256 (6181636)
S33Contrast	26351724 (11642693)	28031059 (30413793)
S33SumOfSqs	31207655 (23581784)	44895214 (30620045)
S33SumEntrp	9666962 (4866084)	11129134 (4721075)
S3m3Contrast	31873105 (27893633)	33185421 (28173496)
S3m3SumOfSqs	35730319 (28691724)	32781770 (23112979)

Table III – Comparison between groups on the left side by using Fisher's exact test or Mann Whitney's test

Parameter	Left Side		P-value
	Control (N=15) Median [Min; Max]	Migraine (N=15) Median [Min; Max]	
Disc Position			0.002
Displaced	1 (6.67%)	10 (66.7%)	
Normal	14 (93.3%)	5 (33.3%)	
Disc Function			0.014
Non-reduced	1 (6.67%)	8 (53.3%)	
Reduced	14 (93.3%)	7 (46.7%)	
S10AngScMom	0.01 [0.01; 0.02]	0.01 [0.01; 0.08]	0.384
S10Contrast	51276596 [2306383; 84148936]	38510638 [0.93; 62234043]	0.071
S10Correlat	0.82 [0.63; 0.91]	0.93 [0.70; 0.97]	<0.001
S10SumOfSqs	15056926 [2569794; 95330325]	40064396 [3164472; 77787772]	0.040
S10SumEntrp	14090097 [1339538;16960223]	15088759 [155121;16127587]	0.373
S01Contrast	31354167 [29375; 87916667]	26052083 [1653125;79895833]	0.576
S01Correlat	0.90 [0.75; 0.96]	0.81 [0.59; 0.89]	<0.001
S01SumOfSqs	18615207 [1392749; 63152751]	41903402 [13801649; 75208333]	0.003
S01SumEntrp	14114043 [1317346;16434899]	14846802 [1588665;16008947]	0.633
S11Contrast	16266667 [9.60; 93444444]	19444444 [21.7; 97222222]	0.885
S11Correlat	0.69 [0.57; 0.83]	0.81 [0.47; 0.93]	0.024
S11SumOfSqs	18923951 [1482358; 93934414]	30792469 [53475; 77865556]	0.152
S11Entropy	19516522 [1887702; 21448948]	20182137 [2056646; 21139066]	0.576
S1m1Contrast	15111111 [17.8; 97777778]	26155556 [28.2; 50811111]	0.820
S1m1Correlat	0.75 [0.50; 0.90]	0.68 [0.46; 0.82]	0.029
S1m1SumOfSqs	17829506 [133275; 99612191]	33312222 [478475; 74592469]	0.101
S20Contrast	24481481 [70.0; 73358025]	17074074 [11481481;50518519]	0.648
S20SumOfSqs	17993484 [1108642; 91769852]	32682061 [4261656; 78595679]	0.085
S02Contrast	18858824 [37.2; 98235294]	60470588 [54.0; 97294118]	0.191
S02SumOfSqs	18021488 [10088249; 59681696]	36974256 [5093564; 74844291]	0.024
S22Contrast	28082192 [2209589; 80589041]	43630137 [4630137; 90136986]	0.101
S22SumOfSqs	23234378 [1921322; 99566523]	38844248 [4343465;78515669]	0.254
S2m2Contrast	23547945 [2930137; 42465753]	27808219 [10027397; 88890411]	0.191
S2m2SumOfSqs	16751783 [4232933; 98084444]	36503847 [2686808; 70033824]	0.290
S30Contrast	41558824 [19.5; 77191176]	33514706 [18.0; 87382353]	0.950
S30SumOfSqs	17217939 [1133045; 89633164]	38455666 [13374946; 78198962]	0.012
S03Contrast	22824324 [1377027; 59324324]	20054054 [10294595; 93972973]	0.576
S03SumEntrp	13000026 [1346483; 15843146]	12934547 [134533; 14577216]	0.263
S33Contrast	35586207 [86.5; 94741379]	65534483 [12262069; 96862069]	0.007
S33SumOfSqs	22688689 [1001843; 93783294]	31782625 [3950379; 77980826]	0.221
S33SumEntrp	12343825 [1213839; 14882474]	12521779 [1378634; 15011721]	0.885
S3m3Contrast	40672414 [3112069; 87431034]	21965517 [10518966; 85655172]	0.373
S3m3SumOfSqs	17316513 [141875; 92875372]	27691439 [2692063; 73344233]	0.494

Table IV – Mean and standard deviation of TA by group on the left side

Parameter	Left Side	
	controlee (N=15)	Migraine (N=15)
	Mean (S.D.)	Mean (S.D.)
S10AngScMom	0.01 (0.00)	0.02 (0.02)
S10Contrast	44301986 (30346039)	28641844 (21966789)
S10Correlat	0.80 (0.08)	0.91 (0.07)
S10SumOfSqs	23528580 (25054501)	39057451 (23520290)
S10SumEntrp	12838915 (4691008)	12867007 (5123403)
S01Contrast	35026681 (29889545)	26651180 (21880585)
S01Correlat	0.89 (0.05)	0.77 (0.09)
S01SumOfSqs	23689571 (15755646)	43688475 (18671290)
S01SumEntrp	12954637 (4798048)	13721724 (3585310)
S11Contrast	33607410 (33125708)	29422964 (27066075)
S11Correlat	0.69 (0.09)	0.78 (0.13)
S11SumOfSqs	28517725 (23414819)	37532854 (24253372)
S11Entropy	16395932 (7490512)	18373084 (4852539)
S1m1Contrast	36976298 (37124643)	24531857 (15028628)
S1m1Correlat	0.74 (0.12)	0.64 (0.11)
S1m1SumOfSqs	26295186 (26423731)	36012836 (21369717)
S20Contrast	24763544 (18766159)	22433745 (10642390)
S20SumOfSqs	26052119 (23656425)	37283380 (22684207)
S02Contrast	37362358 (35096837)	53840004 (30263461)
S02SumOfSqs	23928806 (14270107)	39535013 (21095887)
S22Contrast	32985936 (23918170)	47646575 (25096768)
S22SumOfSqs	34095393 (29117517)	39962861 (22251140)
S2m2Contrast	22687945 (12863432)	37212603 (27577898)
S2m2SumOfSqs	26913427 (24194430)	34259099 (21979002)
S30Contrast	37177259 (23566443)	38783336 (23032607)
S30SumOfSqs	24807160 (23814403)	42007872 (17727533)
S03Contrast	25613423 (18287854)	36822252 (31554449)
S03SumEntrp	12762818 (3341505)	10593494 (5141356)
S33Contrast	33760236 (24282762)	60477241 (26216645)
S33SumOfSqs	29657138 (23455764)	38063010 (23163898)
S33SumEntrp	11087894 (4154230)	10555907 (4902189)
S3m3Contrast	39260345 (25030948)	33853218 (26607776)
S3m3SumOfSqs	25950167 (23550052)	31729412 (24013232)

For analysis of the relationship of the disc position and function with texture parameters, logistic regression models were used for 60 results (two sides *per* patient) in which the comparison was adjusted for side and group. Tables V-VI present the descriptive measurements of the texture parameters by disc position, including *P*-value of the comparison between the positions. It should be observed that this *P*-value is adjusted for side and group only, meaning that the influence of the other two factors on the disc position is not considered.

In Table V, one can observe that individuals with normal disc position had higher values

of entropy for parameters S11Entropy and S03SumEntropy and lower value of contrast for S02Contrast.

Figure 4 shows the texture parameters which present statistically significant differences between the disco positions.

Tables VII-VIII present the descriptive measurements of texture parameters by disc function and the comparison between the disc functions. No statistically significant differences were found between disc functions in relation to the texture parameters.

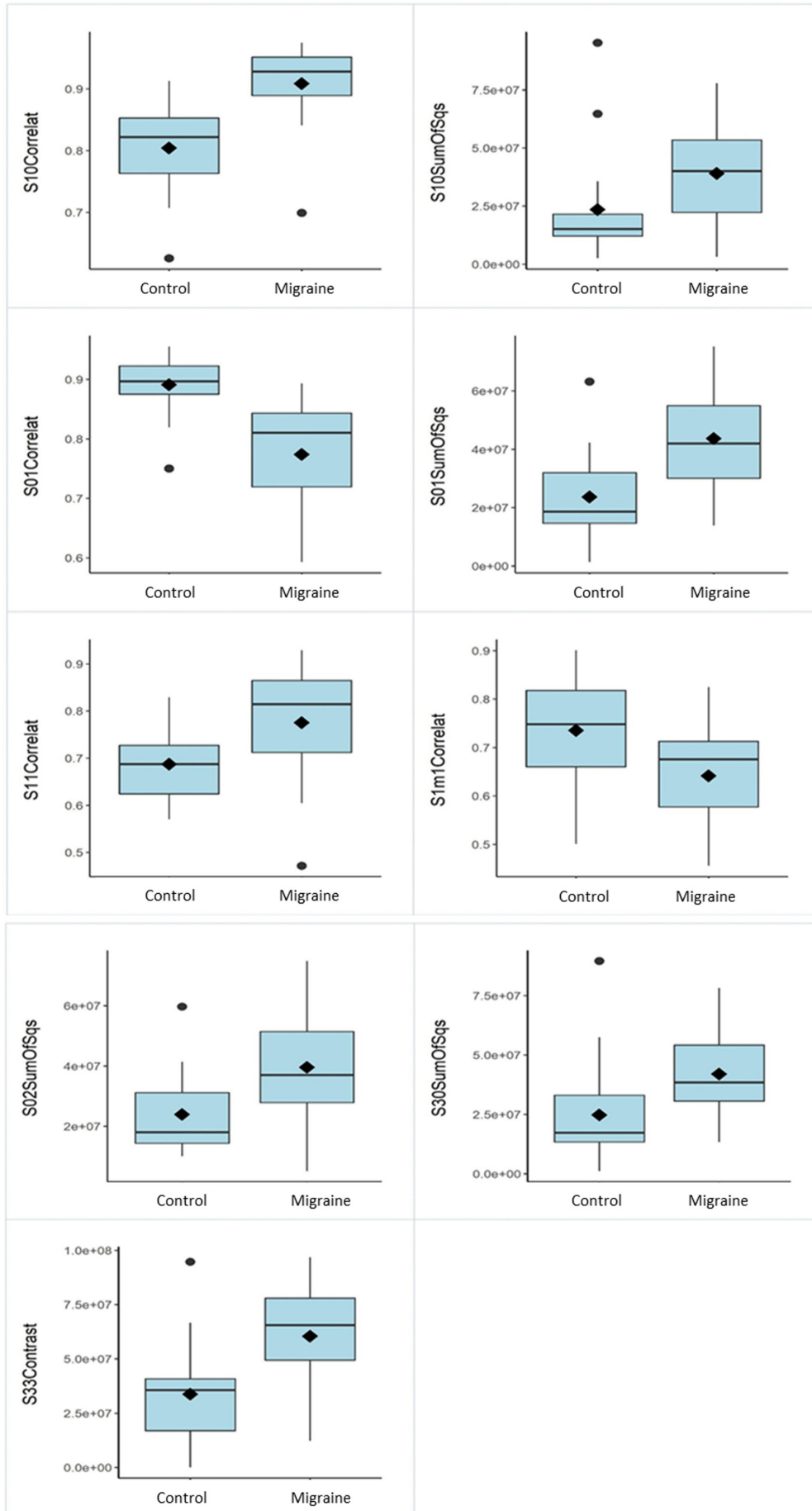


Figure 3 – Boxplots of the texture parameters which presented statistically significant difference between the groups on the left side.

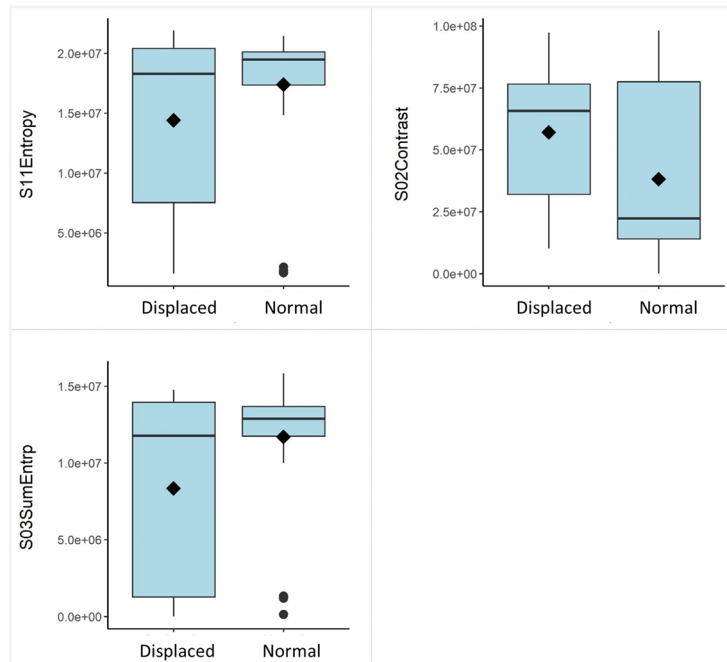


Figure 4 – Boxplots of the texture parameters which presented statistically significant difference between disc positions.

Table V – Comparison between the disc positions by using logistic regression analysis adjusted for side and group

Parameter	Position of the Disc		P-value*
	Displaced (N=23) Median [Min; Max]	Normal (N=37) Median [Min; Max]	
S10AngScMom	0.02 [0.01; 0.10]	0.02 [0.01; 0.08]	0.842
S10Contrast	20319149 [0.53; 62234043]	32021277 [0.93; 84148936]	0.804
S10Correlat	0.92 [0.70; 0.98]	0.86 [0.63; 0.98]	0.527
S10SumOfSqs	40064396 [1432874; 88044364]	19521277 [1889588; 95330325]	0.345
S10SumEntrp	14090097 [0.99; 16572731]	13965937 [1339538; 16960223]	0.320
S01Contrast	22395833 [0.94; 79895833]	28958333 [6.50; 87916667]	0.503
S01Correlat	0.80 [0.59; 0.89]	0.87 [0.64; 0.96]	0.281
S01SumOfSqs	38998671 [151301; 88057454]	20970459 [208294; 75208333]	0.286
S01SumEntrp	14262555 [0.98; 16008947]	13824142 [1273463; 16434899]	0.857
S11Contrast	14444444 [3.10; 82444444]	28444444 [7.10; 97222222]	0.100
S11Correlat	0.77 [0.47; 0.94]	0.74 [0.41; 0.92]	0.508
S11SumOfSqs	39192469 [1136284; 90758025]	22869722 [53475; 93934414]	0.191
S11Entropy	18288017 [1592995; 21917217]	19467541 [1667239; 21448948]	0.025
S1m1Contrast	27977778 [0.83; 76888889]	19744444 [5.40; 97777778]	0.715
S1m1Correlat	0.68 [0.44; 0.82]	0.73 [0.26; 0.90]	0.362
S1m1SumOfSqs	31994321 [66275; 86888889]	20729969 [133275; 99612191]	0.777
S20Contrast	17012346 [1345679; 63209877]	21802469 [70.0; 73358025]	0.293
S20SumOfSqs	31495542 [689148; 88148148]	21879134 [1108642; 91769852]	0.746
S02Contrast	65764706 [10129412; 97294118]	22317647 [4.60; 98235294]	0.041
S02SumOfSqs	36974256 [6843218; 92804498]	20334394 [1380955; 74844291]	0.072
S22Contrast	42054795 [4630137; 88219178]	20849315 [1160274; 90136986]	0.650
S22SumOfSqs	28808032 [2383374; 95241603]	23234378 [1921322; 99566523]	0.489
S2m2Contrast	18219178 [10078082; 88890411]	23479452 [22.0; 62465753]	0.339
S2m2SumOfSqs	36503847 [2781291; 99713361]	19790814 [2032356; 98084444]	0.686
S30Contrast	34088235 [11426471; 87382353]	33264706 [8.50; 90441176]	0.054
S30SumOfSqs	36507299 [6642247; 98234753]	19791306 [1133045; 89633164]	0.220
S03Contrast	16768919 [1177027; 99351351]	23513514 [1377027; 93918919]	0.463
S03SumEntrp	11764806 [0.82; 14758456]	12873781 [136782; 15843146]	0.032
S33Contrast	50862069 [4.50; 96862069]	25689655 [19.5; 94741379]	0.139
S33SumOfSqs	31782625 [3950379; 99912827]	23331971 [1001843; 93783294]	0.847
S33SumEntrp	12012297 [0.78; 15011721]	12343825 [0.82; 14882474]	0.737
S3m3Contrast	19482759 [26.0; 86551724]	32293103 [1912069; 99137931]	0.186
S3m3SumOfSqs	27691439 [2692063; 91964923]	21422934 [119919; 92875372]	0.477

*Adjusted for side and group.

Table VI – Mean and standard deviation of TA by disc position (*Source:* own authorship)

Parameter	Position of the Disc	
	Displaced (N=23)	Normal (N=37)
	Mean (S.D.)	Mean (S.D.)
S10AngScMom	0.03 (0.02)	0.02 (0.01)
S10Contrast	27486587 (21679002)	37436113 (27558505)
S10Correlat	0.89 (0.07)	0.84 (0.09)
S10SumOfSqs	37633606 (26677601)	28385003 (24089053)
S10SumEntrp	12005890 (5537771)	13038230 (3712523)
S01Contrast	23669408 (20608351)	31495130 (25152009)
S01Correlat	0.79 (0.09)	0.85 (0.07)
S01SumOfSqs	39010060 (25254416)	28281069 (20874603)
S01SumEntrp	12515034 (4799391)	12065112 (4901604)
S11Contrast	22028021 (21518303)	37209311 (30663151)
S11Correlat	0.77 (0.11)	0.72 (0.12)
S11SumOfSqs	40350438 (26592918)	30477680 (23968210)
S11Entropy	14408895 (7974506)	17387515 (5657410)
S1m1Contrast	30397105 (20217078)	36241743 (32610271)
S1m1Correlat	0.64 (0.12)	0.70 (0.14)
S1m1SumOfSqs	34885873 (25298199)	31349973 (23871936)
S20Contrast	20483575 (15837016)	25585387 (19045593)
S20SumOfSqs	35297462 (25577973)	31323701 (22434287)
S02Contrast	57069616 (27339067)	38160579 (34247000)
S02SumOfSqs	39614148 (24147140)	28084417 (20046357)
S22Contrast	45757475 (24536921)	30292336 (23776524)
S22SumOfSqs	36798750 (26578718)	33628892 (25580648)
S2m2Contrast	34798273 (27397168)	24494299 (16529478)
S2m2SumOfSqs	38637101 (25726855)	29065364 (22957490)
S30Contrast	44153453 (22705109)	33427985 (24992735)
S30SumOfSqs	42574963 (25676031)	30611179 (21803316)
S03Contrast	34104348 (31481543)	30488897 (23106472)
S03SumEntrp	8342337 (6223982)	11698298 (4003925)
S33Contrast	47025263 (31103351)	31019537 (23057666)
S33SumOfSqs	40799595 (29025107)	32944719 (22922210)
S33SumEntrp	10575789 (4859843)	10631225 (4480825)
S3m3Contrast	29030298 (25652487)	37969851 (26642413)
S3m3SumOfSqs	34400481 (25551685)	29774701 (24112013)

DISCUSSION

Our results indicated that individuals with MH had a higher incidence of changes in the position of articular discs, that is, displaced ones with mouth closed ($P = 0.009$ and $P = 0.002$ for the right and left sides, respectively) in comparison with controls (without MH). In addition, the majority of the discs showed no reduction with maximum mouth opening in these same individuals in view of the changes in disc function ($P = 0.007$ and $P = 0.14$ for the right and left sides, respectively).

This finding did not surprise us, since it is in accordance with other studies [9,10] indicating that MH can be an indicator of temporomandibular dysfunctions related to both masticatory muscles and internal derangements of the articular disc. The issue would involve the assessment of texture parameters of the discs and correlate them to the presence of alterations in patients with MH based on the null hypothesis that articular discs in these individuals would present some differences in the texture values. This would allow us to correlate these parameters to disc displacement and/or

Table VII – Comparison between the disc positions by using logistic regression analysis adjusted for side and group

Parameter	Function of the Disc		P-value*
	Non-Reduced (N=19)	Reduced (N=41)	
	Median [Min; Max]	Median [Min; Max]	
S10AngScMom	0.02 [0.01; 0.10]	0.02 [0.01; 0.08]	0.711
S10Contrast	20319149 [0.53; 62234043]	32021277 [0.93; 84148936]	0.836
S10Correlat	0.92 [0.70; 0.98]	0.86 [0.63; 0.98]	0.239
S10SumOfSqs	40397097 [1432874; 88044364]	19768758 [1889588; 95330325]	0.433
S10SumEntrp	14090097 [0.99; 16572731]	13965937 [1339538; 16960223]	0.177
S01Contrast	22395833 [0.94; 79895833]	28958333 [6.50; 87916667]	0.707
S01Correlat	0.81 [0.66; 0.89]	0.86 [0.59; 0.96]	0.596
S01SumOfSqs	30378228 [151301; 88057454]	23521457 [208294; 75208333]	0.956
S01SumEntrp	14262555 [0.98; 16008947]	13824142 [1273463; 16434899]	0.815
S11Contrast	14444444 [3.10; 82444444]	25566667 [4.00; 97222222]	0.319
S11Correlat	0.78 [0.59; 0.94]	0.73 [0.41; 0.92]	0.708
S11SumOfSqs	39192469 [1136284; 90758025]	23431451 [53475; 93934414]	0.389
S11Entropy	18288017 [1592995; 21917217]	19467541 [1667239; 21448948]	0.171
S1m1Contrast	26333333 [0.83; 76888889]	21122222 [5.40; 97777778]	0.441
S1m1Correlat	0.69 [0.44; 0.82]	0.72 [0.26; 0.90]	0.732
S1m1SumOfSqs	25708025 [478475; 86888889]	23618858 [66275; 99612191]	0.845
S20Contrast	17074074 [1345679; 63209877]	20691358 [70.0; 73358025]	0.374
S20SumOfSqs	22961439 [689148; 88148148]	24086725 [1108642; 91769852]	0.530
S02Contrast	60470588 [10129412; 97294118]	23505882 [4.60; 98235294]	0.463
S02SumOfSqs	37964187 [10332318; 92804498]	21896194 [1380955; 74844291]	0.088
S22Contrast	40958904 [4630137; 88219178]	21890411 [1160274; 90136986]	0.711
S22SumOfSqs	25537249 [2383374; 95241603]	25789454 [1921322; 99566523]	0.902
S2m2Contrast	23547945 [10078082; 88890411]	21945205 [22.0; 68273973]	0.225
S2m2SumOfSqs	30633515 [2781291; 99713361]	21334772 [2032356; 98084444]	0.710
S30Contrast	34088235 [11426471; 87382353]	33264706 [8.50; 90441176]	0.340
S30SumOfSqs	36507299 [11501298; 98234753]	21988754 [1133045; 89633164]	0.166
S03Contrast	24581081 [1177027; 99351351]	22824324 [1377027; 93972973]	0.521
S03SumEntrp	11764806 [0.82; 14758456]	12667773 [136782; 15843146]	0.053
S33Contrast	50862069 [4.50; 96862069]	25689655 [19.5; 94741379]	0.235
S33SumOfSqs	29330187 [3950379; 99912827]	24234468 [1001843; 93783294]	0.949
S33SumEntrp	12012297 [0.78; 15011721]	12343825 [0.82; 14882474]	0.502
S3m3Contrast	21965517 [26.0; 86551724]	29603448 [1912069; 99137931]	0.204
S3m3SumOfSqs	27691439 [6872176; 91964923]	21422934 [119919; 92875372]	0.636

*Adjusted for side and group.

changes in the disc function (i.e. non-reduction), thus working as an auxiliary means to predict these findings.

No study on texture analysis of articular discs of TMJ in individuals with MH was found in the literature. We found a study [22] evaluating the lateral pterygoid muscle in TMJs of patients with TMD by using TA, which was shown to be a very promising technique for identification of parameters indicating changes in these muscles of individuals who have TMD.

Firstly, we analysed the values of texture parameters which were statistically different between control between controls and individuals with MH before evaluating the disc derangements.

Among all the seven texture parameters addressed in the present study, the results showed that there were statistically significant differences ($P < 0.05$) between individuals with MH and controls regarding the parameters Contrast for both right and left sides, with the former presenting higher values of contrast.

Table VIII – Mean and standard deviation of TA by disc function

Parameter	Function of the Disc	
	Non-Reduced (N=19)	Reduced (N=41)
	Mean (S.D.)	Mean (S.D.)
S10AngScMom	0.03 (0.03)	0.02 (0.01)
S10Contrast	26963046 (22915912)	36708044 (26645399)
S10Correlat	0.89 (0.08)	0.85 (0.09)
S10SumOfSqs	37728092 (27579161)	29243520 (24049436)
S10SumEntrp	11569397 (5990785)	13139791 (3563493)
S01Contrast	24136377 (22003432)	30515244 (24363674)
S01Correlat	0.80 (0.07)	0.84 (0.09)
S01SumOfSqs	35801832 (25305987)	30814539 (22079911)
S01SumEntrp	12237826 (5229157)	12237469 (4696687)
S11Contrast	23678363 (22422002)	34963417 (30249391)
S11Correlat	0.79 (0.10)	0.72 (0.12)
S11SumOfSqs	39498146 (25996887)	31835840 (24846656)
S11Entropy	15062162 (7392286)	16794185 (6431425)
S1m1Contrast	28583045 (21623480)	36512196 (31035225)
S1m1Correlat	0.65 (0.13)	0.69 (0.13)
S1m1SumOfSqs	34786664 (25584359)	31740913 (23911341)
S20Contrast	20456075 (15915583)	25100393 (18778918)
S20SumOfSqs	32115929 (26271904)	33185753 (22526148)
S02Contrast	51935046 (27053007)	42384798 (35135353)
S02SumOfSqs	40377609 (24407669)	28855470 (20453156)
S22Contrast	43547080 (23324898)	32825459 (25349461)
S22SumOfSqs	33997994 (27452211)	35236058 (25325930)
S2m2Contrast	36705191 (27582132)	24615871 (17509827)
S2m2SumOfSqs	36333751 (26785819)	31066598 (23216076)
S30Contrast	41412539 (20005099)	35744552 (26381443)
S30SumOfSqs	44117101 (26532841)	31063728 (21658449)
S03Contrast	34236913 (30655525)	30780191 (24565835)
S03SumEntrp	8171181 (6504172)	11450203 (4147384)
S33Contrast	47093013 (30801741)	32549675 (24613418)
S33SumOfSqs	40727816 (29798015)	33744311 (23296334)
S33SumEntrp	10299174 (5295333)	10754004 (4286682)
S3m3Contrast	28224608 (24331018)	37471068 (27109970)
S3m3SumOfSqs	33954923 (23416866)	30432475 (25281251)

A high value of contrast can be interpreted as being the presence of differentiated regions on the image of articular disc, that is, low-signal areas (hyposignal) interspersed among high-signal ones (hypersignal) without a grey-scale gradation which might reduce the contrast (intermediate signals of radiofrequency). Considering that T2-weighted MRI scans were used for calculation of texture parameters of the articular discs, we can infer that high-contrast images as observed by using the TA may be due to the presence of

structural degenerative processes in the articular discs of the individuals with MH. This would lead to deterioration of the normal fibrocartilaginous content, with possible presence of internal hydropic regions, resulting in hypersignal images as liquids have high signals on T2-weighted MRI scans. Interestingly, no region with altered signals was visually found in the image analyses of the articular discs, that is, subjectively. This makes our findings more relevant as they corroborate the hypothesis that the TA can be a mathematic

method allowing the identification of subtle alterations in the structures and which are not evident for a radiologist by means of a simple inspection. It is also important to highlight that, according to the TA, the parameter Contrast does not consist purely of an image histogram, but of statistical calculations for comparing pixel values of adjacent distances, thus allowing the structure to be evaluated as a whole.

A statistical and objective approach for identification of a subtle alteration can be very useful to make a decision regarding the treatment planning and its successful outcome.

A second parameter addressed here was the parameter Correlat (correlation), which was found to have a statistically significant difference ($P < 0.05$) between both groups (controls x individuals with MH). It was observed that individuals with MH had lower values for both right and left sides of the TMJ compared to controls.

In the TA, the parameter Correlat indicates the presence of a grey-scale homogeneity in the image, which is related to the spatial organisation pattern of the tissues [20]. High values of correlation indicate that images are homogeneous, with aligned tissues presenting regular pixel values and uniform distribution patterns without discrepancies. In our study, individuals with MH had lower values of correlation, meaning that the images of their articular disc had a heterogeneous resolution.

Based on the principle that articular discs of TMJ present anterior, intermediate, posterior bands in their normal anatomical aspects in T2-weighted MRI scans with hyposignal intensity, and that this occurs mainly by the linear orientation of the collagen fibres (mainly type I collagen) composing the disc, a lack of homogeneity expressed by the low value of correlation could indicate a disorganization of spatial pattern of these fibres, in addition to areas of hydropic degeneration, as cited before.

The values of the parameters Contrast and Correlat obtained from TA provide information on the composition and structure of the tissue being analysed, respectively, and which are inversely proportional to their values. These findings can be considered as a more specific form of image analysis of the articular discs in MRI scans.

It was found that the parameter SumOfSqs (sum of squares), on the left side, also showed

a statistically significant difference between the groups, with individuals with MH having higher values. According to the TA, the parameter SumOfSqs is related to the variation in the background shades, that is, it is used for differentiating the different anatomical structures within the segmented ROI [21,23]. Because in our study only the articular disc was segmented, this finding is not significant enough as it occurred only on one side. This parameter could indicate that images close to the disc, such as the bilinear zone, whose delimitation with the posterior band is difficult to determine, occasionally could have been included in the ROI. However, in this case, the TA process would exclude these regions from the analyses of other parameters due to the divergent high values found.

Once the behaviours of the texture parameters of the discs have been analysed in the MRI scans, including their meaning, we can discuss the findings on their relationships with the position and function of the articular discs, which is the main objective of this study.

With regard to the position of the articular discs (i.e. normal or displaced), our results indicated that there were statistically significant differences between the parameters Entrp (entropy) ($P = 0.025$), SumEntrp (sum of entropy) ($P = 0.032$) and Contrast (contrast) ($P = 0.041$) for those individuals presenting normal disc position. Also, these individuals have higher values of Entrp and SumEntrp as well as lower values of Contrast compared to individuals with displaced disc.

In general, the parameters Entrp and SumEntrp have a very similar behaviour in the texture analysis, in which the disarray of pixels in the image is analysed first and then the structure of the ROI as a whole [21,24]. A high value of entropy indicates more grey levels in the image, which corresponds to a low contrast [25]. Conversely, when the values of entropy are low, we observed less grey levels and more contrast in the image. These findings are consistent to those previously observed for contrast.

If one considers that normal disc position (high values of Entrp and SumEntrp), and therefore low contrast, was mostly observed in individuals without MH (controls) compared to those with MH, and therefore high contrast, low values of Entrp and SumEntrp should actually indicate the presence of disc displacement

as these parameters behave conversely, as demonstrated by the results for disc position.

These results signal that high values of contrast and low values of entropy (and sum of entropy) can indicate disc displacement in individuals with MH. This was one of our main objectives in the present study.

With regard to the disc function (i.e. reduced or non-reduced), our results indicated that there were no statistically significant differences between the texture parameters and the presence or not of functional reduction of the articular disc.

However, by analysing the tendency of each one of the parameters in relation to the disc function, it was observed that SumEntrp was the only parameter showing a statistical difference between reduced and non-reduced functions (S03) ($P = 0.053$), with the former presenting higher mean values (12667773) compared to the latter (11764806).

This finding is consistent with what has been addressed regarding the position of the articular discs, suggesting that high values of SumEntrp tend to be related to a reduction function antagonistically, whereas low values would be related to a non-reduced function, which was observed in the majority of the individuals with MH. It should be emphasised again that high values of entropy (and sum of entropy) are related to many grey levels, and thus, to a low contrast, whereas low values of entropy are related to high contrast. Once again our results are consistent, since individuals with MH and non-reduced disc (high contrast) should present low entropy, which corroborates the finding on the sum of entropy for reduced disc function.

Nevertheless, some limitations of the present study should be considered, such as the sample size (15 individuals in each group), although previous studies on MRI texture analysis of migraine headache used samples similar to ours and upon which we based our sampling calculation.

We consider that our results are very promising, as they indicate that the MRI texture analysis of articular discs in individuals with MH has the potential to determine the behaviour of the discs in terms of displacement and reduction mainly on the basis of the values of contrast and entropy. Moreover, as this technique is based on contrast and correlation, it can be used as an auxiliary means for identification of subtle

alterations in the composition and structure of articular discs not identified visually in these individuals.

CONCLUSION

The TA of articular discs in individuals with migraine headache has the potential to determine the behaviour of disc derangements based on high values of contrast and low values of entropy, showing that the correlation of these texture parameters can correspond to displacements and a tendency for non-reduction of the discs in these individuals.

Author's Contributions

KACF, CMO, ALFC, TMAMR, ECCBA: Software, Formal analysis, Validation, Investigation, Data Curation, Writing, Review & Editing. SLPCF: Conceptualization, Methodology, Writing, Original Draft Preparation, Supervision, Project administration.

Conflict of Interest

No conflicts of interest declared concerning the publication of this article.

Funding

This study was supported by the São Paulo Research Foundation FAPESP (grant number 2019/22315-0).

Regulatory Statement

This study was conducted in accordance with all the provisions of the local human subjects oversight committee guidelines and policies of: the Institutional Review Board of UNESP. The approval code for this study is: 32339720.8.0000.0077. Informed consent: Written informed consent was obtained from each participant, after informed about the study.

REFERENCES

1. Costa AL, Yasuda CL, Appenzeller S, Lopes SL, Cendes F. Comparison of conventional MRI and 3D reconstruction model for evaluation of temporomandibular joint. *Surg Radiol Anat.* 2008;30(8):663-7. <http://dx.doi.org/10.1007/s00276-008-0400-z>. PMID:18704257.

2. Isberg A. Temporomandibular joint dysfunction : a practitioner's guide. London: CRC Press; 2001. <http://dx.doi.org/10.1201/9780203633151>.
3. Oliveira SSI, Gonçalves SLM, Weig KM, Magalhães TR Fo, Martinez OER, Kalil MTAC, et al. Temporomandibular disorders: guidelines and self-care for patients during Covid-19 pandemic. *Braz Dent Sci*. 2020;23(2):1-8. <http://dx.doi.org/10.14295/bds.2020.v23i2.2255>.
4. Ton LAB, Mota IG, Paula JS, Martins APVB. Prevalence of temporomandibular disorder and its association with stress and anxiety among university students. *Braz Dent Sci*. 2020;23(1):1-9. <http://dx.doi.org/10.14295/bds.2020.v23i1.1810>.
5. Contreras EFR, Fernandes G, Ongaro PCJ, Campi LB, Gonçalves DAG. Systemic diseases and other painful conditions in patients with temporomandibular disorders and migraine. *Braz Oral Res*. 2018;32:e77. <http://dx.doi.org/10.1590/1807-3107bor-2018.vol32.0077>. PMID:30043839.
6. Costa AL, D'Abreu A, Cendes F. Temporomandibular joint internal derangement: association with headache, joint effusion, bruxism, and joint pain. *J Contemp Dent Pract*. 2008;9(6):9-16. <http://dx.doi.org/10.5005/jcdp-9-6-9>. PMID:18784854.
7. Anderson GC, John MT, Ohrbach R, Nixdorf DR, Schiffman EL, Truelove ES, et al. Influence of headache frequency on clinical signs and symptoms of TMD in subjects with temple headache and TMD pain. *Pain*. 2011;152(4):765-71. <http://dx.doi.org/10.1016/j.pain.2010.11.007>. PMID:21196079.
8. Franco AL, Gonçalves DA, Castanharo SM, Speciali JG, Bigal ME, Camparis CM. Migraine is the most prevalent primary headache in individuals with temporomandibular disorders. *J Orofac Pain*. 2010;24(3):287-92. PMID:20664830.
9. Paolo C, D'Urso A, Papi P, Sabato F, Rosella D, Pampa G, et al. Temporomandibular disorders and headache: a retrospective analysis of 1198 patients. *Pain Res Manag*. 2017;2017:3203027. <http://dx.doi.org/10.1155/2017/3203027>. PMID:28420942.
10. Lopes SLPC, Costa ALF, Gamba TO, Flores IL, Cruz AD, Min LL. Lateral pterygoid muscle volume and migraine in patients with temporomandibular disorders. *Imaging Sci Dent*. 2015;45(1):1-5. <http://dx.doi.org/10.5624/isd.2015.45.1.1>. PMID:25793177.
11. Gonçalves DAG, Bigal ME, Jales LCF, Camparis CM, Speciali JG. Headache and symptoms of temporomandibular disorder: an epidemiological study. *Headache*. 2010;50(2):231-41. <http://dx.doi.org/10.1111/j.1526-4610.2009.01511.x>. PMID:19751369.
12. Ballegaard V, Thede-Schmidt-Hansen P, Svensson P, Jensen R. Are headache and temporomandibular disorders related? A blinded study. *Cephalalgia*. 2008;28(8):832-41. <http://dx.doi.org/10.1111/j.1468-2982.2008.01597.x>. PMID:18498400.
13. Larheim TA. Role of magnetic resonance imaging in the clinical diagnosis of the temporomandibular joint. *Cells Tissues Organs*. 2005;180(1):6-21. <http://dx.doi.org/10.1159/000086194>. PMID:16088129.
14. Sano T. Recent developments in understanding temporomandibular joint disorders. Part 1: bone marrow abnormalities of the mandibular condyle. *Dentomaxillofac Radiol*. 2000;29(1):7-10. <http://dx.doi.org/10.1038/sj.dmf.4600492>. PMID:10654030.
15. Lubner MG, Smith AD, Sandrasegaran K, Sahani DV, Pickhardt PJ. CT texture analysis: definitions, applications, biologic correlates, and challenges. *Radiographics*. 2017;37(5):1483-503. <http://dx.doi.org/10.1148/rg.2017170056>. PMID:28898189.
16. Raja JV, Khan M, Ramachandra VK, Al-Kadi O. Texture analysis of CT images in the characterization of oral cancers involving buccal mucosa. *Dentomaxillofac Radiol*. 2012;41(6):475-80. <http://dx.doi.org/10.1259/dmfr/83345935>. PMID:22241875.
17. Albuquerque M, Anjos LG, Andrade HMT, Oliveira MS, Castellano G, Rezende TJR, et al. MRI texture analysis reveals deep gray nuclei damage in amyotrophic lateral sclerosis. *J Neuroimaging*. 2016;26(2):201-6. <http://dx.doi.org/10.1111/jon.12262>. PMID:26011757.
18. Headache Classification Subcommittee of the International Headache Society. The International Classification of Headache Disorders: 2nd edition. *Cephalalgia*. 2004;24(Suppl 1):9-160. PMID:14979299.
19. Tasaki MM, Westesson PL, Isberg AM, Ren YF, Tallents RH. Classification and prevalence of temporomandibular joint disk displacement in patients and symptom-free volunteers. *Am J Orthod Dentofacial Orthop*. 1996;109(3):249-62. [http://dx.doi.org/10.1016/S0889-5406\(96\)70148-8](http://dx.doi.org/10.1016/S0889-5406(96)70148-8). PMID:8607470.
20. Pinto GNS, Grossmann E, Iwaki L Fo, Groppo FC, Poluha RL, Muntean SA, et al. Correlation between joint effusion and morphology of the articular disc within the temporomandibular joint as viewed in the sagittal plane in patients with chronic disc displacement with reduction: a retrospective analytical study from magnetic resonance imaging. *Cranio*. 2021;39(2):119-24. <http://dx.doi.org/10.1080/08869634.2019.1582166>. PMID:30786838.
21. Oliveira MS, Fernandes PT, Avelar WM, Santos SL, Castellano G, Li LM. Texture analysis of computed tomography images of acute ischemic stroke patients. *Braz J Med Biol Res*. 2009;42(11):1076-9. <http://dx.doi.org/10.1590/S0100-879X2009005000034>. PMID:19820884.
22. Fan WP, Liu MQ, Zou Y, Wang X, Wang PH, Chen ZY. MRI histogram texture analysis of lateral pterygoid muscle in patients with temporomandibular disorders. *Zhonghua Kou Qiang Yi Xue Za Zhi*. 2020;55(12):963-8. PMID:33280361.
23. Ganeshan B, Miles KA, Young RC, Chatwin CR. Texture analysis in non-contrast enhanced CT: impact of malignancy on texture in apparently disease-free areas of the liver. *Eur J Radiol*. 2009;70(1):101-10. <http://dx.doi.org/10.1016/j.ejrad.2007.12.005>. PMID:18242909.
24. Haralick RM, Shanmugam K, Dinstein IH. Textural features for image classification. *IEEE Trans Syst Man Cybern*. 1973;SMC-3(6):610-21. <http://dx.doi.org/10.1109/TSMC.1973.4309314>.
25. Gonçalves BC, Araújo EC, Nussi AD, Bechara N, Sarmento D, Oliveira MS, et al. Texture analysis of cone-beam computed tomography images assists the detection of furcal lesion. *J Periodontol*. 2020;91(9):1159-66. <http://dx.doi.org/10.1002/JPER.19-0477>. PMID:32003465.

Sérgio Lucio Pereira de Castro Lopes
(Corresponding address)

Universidade Estadual Paulista, Instituto de Ciência e Tecnologia,
Departamento de Diagnóstico e Cirurgia, Av. Eng. Francisco José Longo, 777 -
Jardim São Dimas, CEP 12245-000, São José dos Campos, SP, Brasil.
E-mail: sergio.lopes@unesp.br

Date submitted: 2022 Oct 04
Accept submission: 2022 Dec 16